Scientia Iranica D (2014) 21(3), 924–934

SCIENTIA IRANICA

Sharif University of Technology

Scientia Iranica

Transactions D: Computer Science & Engineering and Electrical Engineering

www.scientiairanica.com

Incorporating large photovoltaic farms in power generation system adequacy assessment

A. Ghaedi, A. Abbaspour, M. Fotuhi-Friuzabad* and M. Parvania

Center of Excellence in Power System Control and Management, School of Electrical Engineering, Sharif University of Technology, Tehran, P.O. Box 11365-11155, Iran.

Received 20 April 2013; received in revised form 11 August 2013; accepted 27 October 2013

KEYWORDS

Adequacy assessment; Photovoltaic farm; Reliability model; Solar radiation uncertainty.

Abstract. Recent advancements in photovoltaic (PV) system technologies have decreased their investment cost and enabled the construction of large PV farms for bulk power generations. The output power of PV farms is affected by both failure of composed components and solar radiation variability. These two factors cause the output power of PV farms be random and different from that of conventional units. Therefore, suitable models and methods should be developed to assess different aspects of PV farms integration into power systems, particularly from the system reliability viewpoint. In this context a reliability model has been developed for PV farms with considering both the uncertainties associated with solar radiation and components outages. The proposed model represents a PV farm by a multi-state generating unit which is suitable for the generation system assessment. Utilizing the developed reliability model, an analytical method is proposed for adequacy assessment of power generation systems including large PV farms. Real solar radiation data is used from Jask region in Iran which are utilized in the studies performed on the RBTS and the IEEE-RTS. Several different analyses are conducted to analyze the reliability impacts of PV farms integration and to estimate the capacity value of large PV farms in power generation systems.

1. Introduction

In recent years, renewable generations, especially wind power and photovoltaic (PV) systems, have been increasingly used in power systems. The non-exhaustive nature of renewable resources, along with negligible operating costs and benign environmental effects, are primary benefits in power system applications. Recent advancements in PV system technology have decreased the investments costs of PV systems. Although the cost of power produced by PV systems is still higher than the same size conventional generations, and they normally require additional facilities to integrate and transfer the power to the grid, they are supported strongly by governmental policies in order to reduce harmful emissions. The Renewable Portfolio Standards (RPSs), Renewable Energy Certificates (RECs) [1], and regional greenhouse gas emission control schemes [2] in the US, and the 20/20/20 targets in the European Union [3], are examples of such policies. The ultimate target of these policies is to increase the use of renewable energy and reduce environmental emissions. The 250 MW Agua Caliente Solar plant in the USA, the 214 MW PV Charanka powerplant in India and the 200 MW Yuma County PV powerplant in the USA are examples of such PV farms that have been constructed around the world in the past two years [4].

The intermittent nature of solar radiation, along with the probabilistic behavior of PV farm compo-

*. *Corresponding author. Tel: +98 21 66165921*
E-mail addresses: ghaedi@ee.sharif.edu (A. Ghaedi); abbaspour@sharif.edu (A. Abbaspour); fotuhi@shairf.edu (M. Fotuhi-Friuzabad); parvania@ee.sharif.edu (M. Parvania)

nent outages, makes the output power of PV farms completely random and different from conventional generation units. Therefore, new models and methods are required to assess the different aspects of PV farm integration in power systems, particularly from the system reliability point of view. Very little attention has been paid to assessing the power system reliability impact of PV farm integration. In [5], the hourly mean solar radiation and standard deviation are applied as inputs to simulate solar radiation over a year. Then, the Monte Carlo simulation technique is utilized for reliability analysis of a small isolated power system containing solar photovoltaic. A time sequential simulation method is proposed in [6] for generating the capacity adequacy evaluation of small stand-alone power systems containing solar energy, operating in parallel with battery storage. The system considered in [6] is composed of a diesel generator, a PV system, and battery storage. In [7] and [8], a reliability evaluation of isolated power systems containing a PV system and wind generation is studied. In those papers, the capacity of renewable resources is assumed to be small and the Monte Carlo method is used for the uncertainty modeling of wind speed and solar radiation. In [9], a reliability study of a hybrid system containing wind and solar generation in off-grid applications of a real system is performed. Various reliability indices, such as loss of load expectation, expected energy not served, energy index of reliability and expected customer interruption cost, are evaluated through a probabilistic approach using an analytical method. In [10], a reliability analysis of a hybrid wind and solar system, based on a well-being approach, which is a combination of probabilistic and deterministic techniques, is performed thorough a Monte Carlo simulation technique. The Monte Carlo simulation method is used in [11] for the reliability evaluation of a hybrid system containing wind and PV systems connected to multi micro storage systems. All the references have considered the reliability impact of PV farm integration in isolated power systems. In this context, an analytical method is proposed in this paper for the adequacy assessment of power generation systems, including large PV farms. A reliability model is first developed for PV farms, which considers both the uncertainties associated with solar radiation and component outages. The proposed reliability model represents a PV farm via a multi-state generating unit, which makes it easy to be utilized in the generation system reliability assessment. The developed multi-state reliability model is utilized to form a Capacity Outage Probability Table (COPT) of the PV farm(s). The obtained COPT is then added to the equivalent COPT of the conventional generating units to form the total generation capacity model of the system. Finally, convolution of the load model with the final COPT provides the risk model of the generation system, including PV farms, and the reliability indices can be calculated using the obtained risk model. The proposed analytic approach overcomes some of the difficulties associated with simulation-based methods, in terms of both computational burden and the volume of data needed in such methods. Besides, the proposed analytic model can be used in generation system expansion planning, including large PV farms.

The rest of the paper is organized as follows. A typical structure of a PV farm considered in this paper is presented in Section 2. In Section 3, the proposed component reliability model for PV farms is presented. The model proposed in Section 3 is then modified in Section 4, in order to consider the effect of solar radiation uncertainties. The real solar radiation data in the southern part of Iran is utilized in Section 4. The proposed analytic method for the adequacy assessment of power systems, including PV farms, is presented in Section 5. The proposed model is applied to the RBTS and the IEEE-RTS in Section 6, to analyze the reliability impact of PV farm integration in power systems. Finally, conclusions are given in Section 7.

2. PV farm structure

The structure of a typical PV farm is shown in Figure 1 [12]. The smallest building block of a PV farm is the solar cell, which absorbs the solar radiation and converts it to the DC electric power. A number of solar cells are connected in series and in parallel to construct a PV panel and achieve larger current-voltage characteristics. The output power of a solar panel is maximized in a point named the Maximum Power Point (MPP). A number of solar panels are then connected to a DC/DC converter to target the MPP and yield the maximum power produced by the panels. This DC/DC converter is usually known as the MPP Tracker (MPPT) [12]. Such a structure consists of solar panels connected to a DC/DC converter, which is usually known as a PV sub-array. The power produced by a sub-array is still DC. In order to connect the

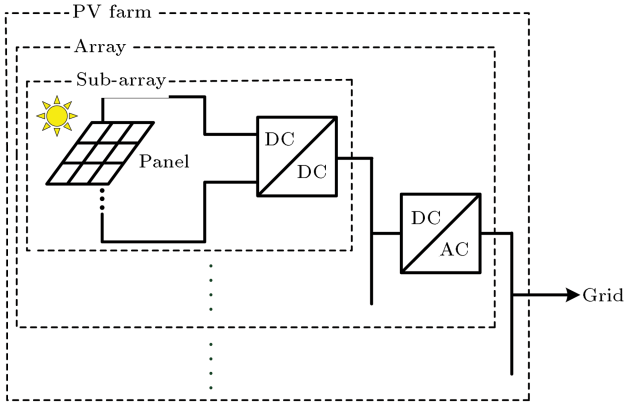

Figure 1. The structure of a typical PV farm.

PV farm to the AC grid, some sub-arrays are then connected to a DC/AC converter to construct a PV array, which is the largest building block of a PV farm.

In order to provide a better representation of the proposed reliability model, a 30 MW PV farm is utilized throughout the paper. Each panel of the sample PV farm includes 96 solar cells in three 32-cell branches. The maximum output power of a panel in the presence of 900 watt/m^2 solar radiation is 300 watts. This value is resulted from the product of the area of the panel (2 m^2), panel efficiency (18.4%), the efficiency of other parts, such as connecting wires and converters (90%), and solar radiation [13]. In the considered PV farm, a sub-array includes 40 series panels connected to a 12 kW DC/DC converter for maximum power point tracking. At a higher level, a PV array with a capacity of 600 kW is constructed from 50 parallel sub-arrays. This array is connected to the AC grid through a 600 kW inverter. Finally, 50 PV arrays are connected in parallel to construct a 30 MW PV farm.

3. Component reliability modeling of a PV farm

A component reliability model of a large PV farm connected to the AC grid is presented in this section. The modeling is commenced by presenting the reliability model of a solar cell, and is then extended to a PV panel, a PV sub-array, a PV array and, finally, the PV farm.

3.1. Reliability model of a solar cell

A solar cell is a p-n junction which produces DC electricity power from sun radiation [12]. A two-state up and down model is considered as the reliability model of a solar cell. The failure of solar cells could originate from electrical, chemical, environmental and mechanical phenomena, such as thermal stresses, humidity penetration and solid state failures [14]. The probabilities of the up and down states can be calculated as follows [15]:

$$P_c^{\mathrm{UP}} = \frac{\mu_c}{\lambda_c + \mu_c}, \qquad P_c^{\mathrm{DOWN}} = \frac{\lambda_c}{\lambda_c + \mu_c}, \tag{1}$$

where λ_c and μ_c are failure rate and repair/replacement rate of a solar cell, respectively. Failure rate and repair time of the p-n junction of a solar cell of the considered 30 MW PV farm are considered to be 0.005 failures in 10^6 hours (0.00004 f/yr) and 40 hours, respectively [16].

3.2. Reliability model of a PV panel

A PV panel is constructed by M parallel branches, each with N series solar cells. If a solar cell fails, the associated branch would go out of service. Accordingly, the failure rate of a branch is the sum of the failure rate of the series solar cells [17]. Thus, the probabilities of the up and down states of a panel branch can be calculated by Eqs. (2), respectively:

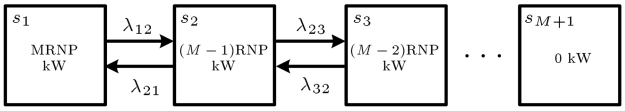

Figure 2. Reliability model of a PV sub-array.

$$P_b^{\mathrm{UP}} = \frac{\mu_b}{\lambda_b + \mu_b} = \left(P_c^{\mathrm{UP}}\right)^N,$$

$$P_b^{\mathrm{DOWN}} = \frac{\lambda_b}{\lambda_b + \mu_b} = 1 - P_b^{\mathrm{UP}}, \tag{2}$$

where λ_b and μ_b are failure rate and repair/replacement rate of a branch, respectively. Using the principles of series systems [15], λ_b and μ_b are equal to $N\lambda_c$ and μ_c, respectively.

3.3. Reliability model of a PV sub-array

In a PV panel with M parallel branches, the failure of a branch reduces the output power of the panel to the $(M-1)/M$ maximum power output of the panel. As the direct consequence of this failure, and based on Kirchhoff's current law, the current of the other panels must be reduced by a factor of $(M-1)/M$. Thus, the total output power of the sub-array would be reduced to $(M-1)/M$ times nominal power. The reliability model of a PV sub-array is shown in Figure 2, with $(M+1)$ states. In Figure 2, P is the power produced by each solar cell, N is the number of series cells in a branch, M is the number of parallel branches in a panel, and R is the number of series PV panels in a sub-array.

The state probabilities in Figure 2 can be calculated as follows.

In state s_1, all branches and panels are in service. The total number of branches is MR. Thus, the probability of residing in this state can be calculated as follows:

$$P_{s_1} = \left(P_b^{\mathrm{UP}}\right)^{MR}. \tag{3}$$

The probability of residing in state s_2 is a summation of the state probabilities in which there is at least a panel with one failed branch. In this state, there is no panel with two or more failed branches, but the number of panels with one failed branch can be one or more. This state contains R sub states with one to R panels, containing one failed branch. Thus P_{s_2} is:

$$P_{s_2} = \sum_{k=1}^{R} \left(M^k \binom{R}{k} \left(P_b^{\mathrm{UP}}\right)^{MR-k} \left(P_b^{\mathrm{DOWN}}\right)^k \right). \tag{4}$$

In Eq. (4), k is the number of panels with one failed branch. A sub array contains R panels, each with M branches. The total number of options, i.e. the number

of states containing k panels with one failed branch, would be the combination k from R multiplied by M^k.

The probability of residing in state s_3 is equal to the summation of state probabilities in which there exists at least a panel with exactly two failed branches. In this state, there is no panel with three or more failed branches, but the number of panels with two failed branches (k) can be one or more (up to R). Also, the number of panels with one failed branch from the other panels (h), can be from zero to ($R-k..$). Thus, the probability, P_{s_3}, is calculated as:

$$P_{s_3} = \sum_{k=1}^{R} \sum_{h=0}^{R-k} \left[\binom{R}{k} \binom{R-k}{h} \binom{M}{2}^k M^h \left(P_b^{\mathrm{UP}}\right)^{RM-2k-h} \left(P_b^{\mathrm{DOWN}}\right)^{2k+h} \right]. \quad (5)$$

The remaining state probabilities in Figure 2 can be calculated in the same way. The transition rates between states in Figure 2 can be calculated using the same analysis. The capacity of the sub-array in Figure 2 decreases from $MRNP$ kW to $(M-1)RNP$ kW when one of the branches in a panel fails. Thus, the transition rate from state s_1 to state s_2 is occurred when one of the RM branches fails, and is:

$$\lambda_{12} = RM\lambda_b. \quad (6)$$

The sub-array is transferred from state s_2 to state s_1 when the only failed branch is replaced or repaired. This transition occurs when there is a state with only one failed branch. The equivalent transition rate is calculated based on the frequency balance of the same states. Thus:

$$\lambda_{21} = \frac{\mu_b RM \left(P_b^{\mathrm{UP}}\right)^{MR-1} P_b^{\mathrm{DOWN}}}{P_{s_2}}. \quad (7)$$

In Eq. (7), $RM(P_b^{\mathrm{UP}})^{MR-1}P_b^{\mathrm{DOWN}}$ is the probability of the state with only one failed branch.

The sub-array in state s_2 has at least one panel with one failed branch. If the other healthy branch(es) of the panel(s) with one failed branch fails, the sub-array would go to state s_3. It is considered that, in state s_2, there are k panels with one failed branch. Thus, if a branch of the remaining $(M-1)$ perfect branches fails, the transition is occurred. Accordingly, using the rule of the combining failure rate of the same states [15], the transition rate from state s_2 to state s_3 can be calculated by:

$$\lambda_{23} = \frac{\sum_{k=1}^{R} \left[(M-1)k\lambda_b M^k \binom{R}{k} \left(P_b^{\mathrm{UP}}\right)^{MR-k} \left(P_b^{\mathrm{DOWN}}\right)^k \right]}{P_{s_2}}. \quad (8)$$

In Eq. (8), $(M-1)k\lambda_b$ is the transition rate associated with the states containing k panels with one failed branch, and $M^k \binom{R}{k} (P_b^{\mathrm{UP}})^{MR-k}(P_b^{\mathrm{DOWN}})^k$ is the probability of these states.

The sub-array in state s_3 has one or more panels with two failed branches. But, the sub-array can go from state s_3 to state s_2, if and only if it has one panel with two failed branches. By repairing/replacing one of the failed branches of the panel, the sub-array would be transferred to state s_2. Thus, as in Eq. (9), shown in Box I, $2\mu_b$ is the transition rate associated with the states containing one panel with two failed branches. In these states, the remaining panels may have one failed branch or not, i.e. the number of panels with one failed branch may be $0, 1 \cdots (R-1)$. In Eq. (9), shown in Box I, R is the number of options, determining a panel with two failed branches, $\binom{M}{2}$ is the number of options determining two failed branches from M branches of a panel, and $M^k \binom{R-1}{k} (P_b^{\mathrm{UP}})^{MR-k-2}(P_b^{\mathrm{DOWN}})^{k+2}$ is the probability of states containing one panel with two failed branches incorporating K panels with one failed branch.

The remaining transition rates in Figure 2 can be calculated in the same way. For example, in the considered 30 MW PV farm, when a branch of a panel consisting of three branches fails, the output power of the panel reduces to 2/3 the maximum output power of the panel. Accordingly, the output power of the sub-array would have four states, i.e. 12, 8, 4 and 0 kW. The state probabilities and the associated transition rates can be calculated using the above procedure. Besides the failures originated by the solar cells failures, the panels and the associated sub-arrays may also fail due to a common mode failure. In such failures, which

$$\lambda_{32} = \frac{2\mu_b \sum_{k=0}^{R-1} \left[R \binom{M}{2} M^k \binom{R-1}{k} \left(P_b^{\mathrm{UP}}\right)^{RM-k-2} \left(P_b^{\mathrm{DOWN}}\right)^{k+2} \right]}{P_{s_3}}. \quad (9)$$

Box I

normally happen due to storm, snow, wind blowing, panel basement breaking, etc., the whole panel and, thus, the whole sub-array would fail. Considering the common mode failures, the reliability model of the sub-array shown in Figure 2 would be extended to the model in which a transition is made from each state to a 0 kW capacity state, which denotes the common mode failure of the panel. The common mode failure state probabilities can be calculated using the frequency balance principle [15].

As shown in Figure 1, the panels in a sub-array are connected to a DC/DC converter for maximum power point tracking. The next step in the reliability modeling of a sub-array is to consider the failure of the DC/DC converter. From the reliability modeling point of view, the DC/DC converter is in series with all the panels in a sub-array and its failure results in the failure of the whole sub-array. Hence, failure of the DC/DC converter can be considered as a common mode failure and can be evaluated using the same procedure utilized above to model the common mode failures. The DC/DC converter can be modeled using a simple two-state up and down reliability model. Accordingly, a reliability model of the sub-array of a sample 30 MW PV farm, which accounts for common mode failures and the failure of the DC/DC converter, is shown in Figure 3. The new state probabilities and transition rates are also shown in this figure.

The common mode failure rate and repair/replacement rate of a panel of the 30 MW PV farm are assumed to be 0.004 f/yr and 219 r/yr, respectively. The failure rate and repair/replacement rate of the DC/DC converter are also considered to be 0.01 f/yr and 219r/yr, respectively.

3.4. Reliability model of a PV array

A PV array consists of L parallel sub-arrays. From a reliability point of view, L sub-arrays are in parallel, each modeled by a $(M+1)$-state model derived in Section 3.3. Consequently, the reliability model of a PV

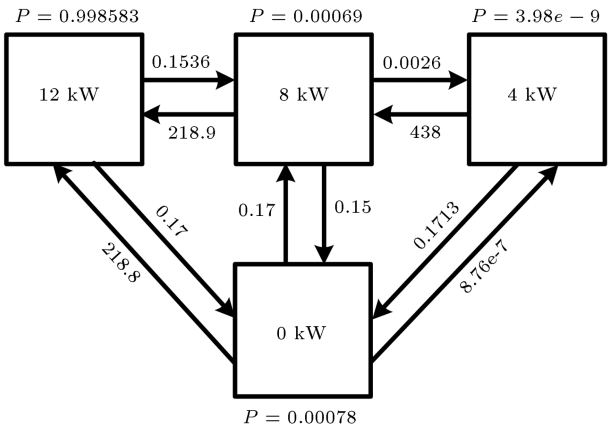

Figure 3. Reliability model of a sub-array of the 30 MW PV farm.

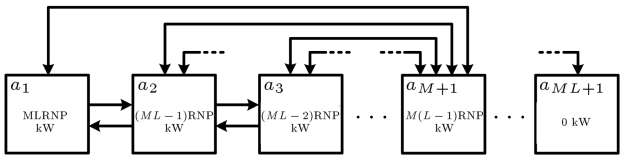

Figure 4. Reliability model of a PV array.

array, shown in Figure 4, consists of $(ML+1)$ states, from $MLRNP$ kW to 0 kW capacities, reducing in RNP kW steps. The state probabilities and transition rates in Figure 4 can be calculated in a straightforward manner by investigating the sub-array failure states. For example, in state a_1, all sub-arrays are in state s_1. Hence, the probability of residing in state a_1 is:

$$P_{a_1} = (P_{s_1})^{ML}. \tag{10}$$

In the sample 30 MW PV farm, 50 parallel sub-arrays construct a PV array. Thus, the nominal output power of an array of the PV farm would be 600 kW. Consequently, the reliability model of each PV array consists of 151 states, from 600 kW to 0 kW capacities, reducing in 4 kW steps. However, this model contains a large number of states for a PV array, which is not desirable for reliability studies. Hence, the output power of a PV array is approximated by an arbitrary number of states. For example, the 151-state model of each array in the 30 MW PV farm is approximated by seven states with 600, 500, 400, 300, 200, 100 and 0 kW capacities. This model is constructed through state 1 with capacities from 552 to 600 kW, state 2 with capacities from 452 to 548 kW, state 3 with capacities from 352 to 448 kW, state 4 with capacities from 252 to 348 kW, state 5 with capacities from 152 to 248 kW, state 6 with capacities from 52 to 148 kW and state 7 with capacities from 0 to 48 kW. The state probabilities of the approximated 7-state model are obtained by summing up the probability of the associated states in the complete 151-state reliability model of the PV array.

3.5. Reliability model of a PV farm

A DC/AC converter is in series with each PV array to transfer the produced power to the grid, and its failure causes the output power of the associated array to be zero. Similar to the method utilized to model the failure of the DC/DC converter in each sub-array, failure of the DC/AC converter can be considered as a common mode failure and can be evaluated using the same procedure. Accordingly, a transition is made from each state of Figure 4 to a 0 kW capacity state, which denotes the failure of the DC/AC converter. The transition rates to/from the new states with 0 kW capacities are the failure rate/repair rate of the DC/AC converter. The resulting reliability model of each array, considering the DC/AC converter, is similar to the model shown in Figure 4, with $(ML+1)$ states in

which the state probabilities and transition rates are updated.

Consider a PV farm with G parallel arrays. From a reliability point of view, G arrays (each in series with a DC/AC converter) are in parallel, and each are modeled by a $(ML+1)$-state model. Accordingly, the reliability model of a PV farm consists of $(MLG+1)$ states, from $MLGRNP$ kW to 0 kW capacities, reducing by RNP kW steps. In this regard, based on the 7-state reliability model of each array of the sample 30 MW PV farm derived in Section 3.4, which is further manipulated to include the failure of the DC/AC converter, the reliability model of a 30 MW PV farm consisting of 50 parallel arrays would have 301 states. However, this large number of states is not suitable for reliability analysis of power systems. Investigating the 7-state model derived in Section 3.4 reveals that the probabilities associated with states of 500, 400, 300, 200, 100 and 0 kW capacities are, respectively, 3.174e-9, 1.567e-29, 3.58e-52, 7.36e-79, 1.088e-107 and 2.497e-138, which are almost zero and can be omitted from the model. Thus, without losing the precision of calculations, the reliability model of the PV array of a 30 MW PV farm can be best approximated by only one state having 600 kW capacity and unity probability.

Considering the two-state reliability model for the DC/AC converters, we can derive a 51-state reliability model for the sample 30 MW PV farm. The failure and repair rates of the DC/AC converters are 0.5 f/yr and 50 r/yr, respectively. We can simplify the model by clustering the states into 4 states, with 30, 20, 10 and 0 MW capacities. This model is constructed through state 1 with capacities from 25.2 to 30 MW, state 2 with capacities from 15 to 24.6 MW, state 3 with capacities from 5.4 to 14.4 MW, and state 4 with capacities from 0 to 4.8 MW.

4. Solar radiation uncertainty considerations in reliability model of PV farms

Besides the random nature of components in a PV farm, the solar radiation is also uncertain and can considerably affect the output power of the farm. Every physical event, such as solar radiation, that changes continuously and randomly in time and space, is considered a stochastic process and can be modeled approximately as a process with discrete state space and relevant parameters [18]. A Markov chain may be used to model the alteration of a stochastic process as transitions between states, where each state represents a discrete value of the process. As a basic characteristic of the Markov process, it should be stationary, i.e. the transition rates between different states should remain constant through the study period [19]. Modeling a stochastic process by a stationary Markov process demands that the state residence time follows an exponential distribution [17]. In this paper, exponential state residence time is assumed for all applications. In exponential distribution, a constant transition rate between states i and j is used, which is defined by [17]:

$$\lambda_{ij} = \frac{N_{ij}}{T_i}, \tag{11}$$

where λ_{ij} is the transition rate (occurs per hour), N_{ij} is the number of observed transitions from state i to state j, and T_i is the duration of state i (in hours) calculated during the whole period. If the departure rates from state i to the upper and lower states are denoted as λ_{+i} and λ_{-i}, respectively, then [17]:

$$\lambda_{+i} = \sum_{j>i} \lambda_{ij}, \tag{12}$$

$$\lambda_{-i} = \sum_{j<i} \lambda_{ij}. \tag{13}$$

The probability of occurrence of state i, P_i, is given by [17]:

$$P_i = \frac{T_i}{T}, \tag{14}$$

where T is the entire period of observation (in hours). The frequency of occurrence of state i, f_i (in occurrences per hour), is then given by [17]:

$$f_i = P_i(\lambda_{+i} + \lambda_{-i}). \tag{15}$$

The output power of a PV farm at a definite time can be estimated using the solar radiation data. We have utilized the yearly solar radiation data of the Jask region in the southern part of Iran [20], to obtain the output power of the considered 30 MW PV farm for a year-long horizon. However, the amount of solar radiation data and the associated output power states of the PV farms is too large, which is not suitable for the analytical reliability evaluation of a power system, unless the amount of data is reduced by a clustering method.

To attain a proper Markov model for the PV farm, its output power should be split up to some finite states. To find the number and range of these steps, an efficient clustering method, which could simultaneously guarantee model accuracy and generality, has to be employed. Clustering is a process for classifying patterns or objects in such a way that samples of the same group are more similar to one another than samples belonging to different groups. Many clustering approaches with special characteristics, such as hard clustering and fuzzy clustering schemes, have been introduced in the literature. The conventional hard clustering approach restricts each point of the data set to, exclusively, just one cluster. As a consequence, with this technique, the segmentation results are often very crisp. However, in many real situations, issues such as limited spatial resolution, poor contrast and overlapping intensities

make this hard segmentation a difficult task. The other clustering approach, i.e. fuzzy clustering, as a soft segmentation method has been widely studied and successfully applied to image segmentation. Among the fuzzy clustering methods, the Fuzzy C-Means (FCM) algorithm is the most popular method used in image segmentation, due to its robust characteristics for ambiguity, and its capability of retaining much more information than hard segmentation methods [21].

In this paper, we have employed the Fuzzy C-Means (FCM) clustering method as a robust method in dealing with structure identification of unlabeled data [22]. Employing this method, object data $X = [x_1, x_2, \cdots, x_n]$ can be categorized into m clusters minimizing the following objective function [22]:

$$J_m(U, v) = \sum_{i=1}^{m} \sum_{k=1}^{n} U_{ik}^{f} \left| x_k - v_k \right|, \tag{16}$$

where f, v_k and U_{ik} are, respectively, the fuzzification parameter, the center of the ith cluster and the fuzzy degree between x_k and the ith cluster. This FCM technique is implemented on the historical output power data of the sample 30 MW PV farm and, then, the number and probability of the cluster centers are specified, which represent the various states associated with the PV farm generation levels. By increasing the number of associated clusters, the value of the objective function decreases. As shown in Figure 5, decrement in the objective function becomes insignificant when the number of considered clusters is seven or more. So, it can be concluded that a seven-cluster model can be regarded as a proper one for the PV farm. The resulting seven clusters are presented in Table 1. Once the output power has been split into finite steps by FCM, the various attributes associated with these states, i.e. transition rates between different states, and state probabilities and frequencies, can be calculated. Consequently, the reliability model of the 30 MW PV farm, considering variability in solar radiation, can be obtained, which is presented in Table 2. The transition rates between states in the model can be calculated by Eq. (11) to develop the transition matrix shown in Box II.

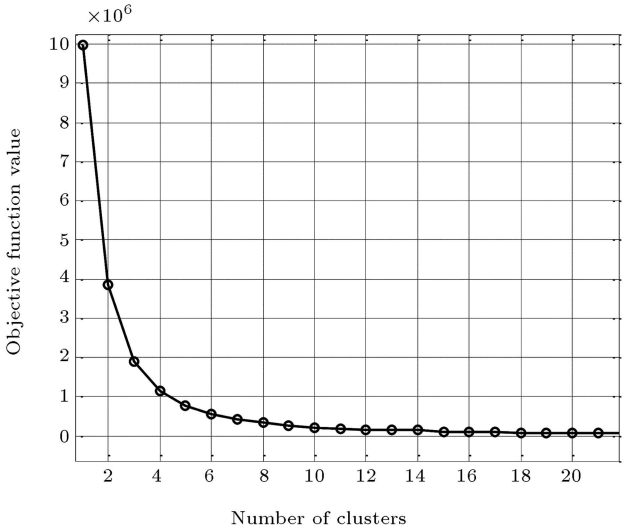

Figure 5. The value of the FCM objective function with respect to the number of states.

Table 1. Clustering of PV farm output powers.

Cluster number	Cluster center (MW)	Cluster range (MW)
1	29.8	28.2-30
2	26.4	24.7-28.2
3	22.9	20.5-24.7
4	18	14.8-20.5
5	11.6	8.7-14.8
6	5.9	3-8.7
7	0	0-3

The 4-state component reliability model of the 30 MW PV farm derived in Section 3.5, can be combined with the 7-state Markov model of Table 2 to form the complete reliability model of the PV farm. The resulting 19-state model, presented in Table 3, accounts for both the component availability of the PV farm and solar radiation uncertainty.

5. Adequacy assessment of power generation system including PV farms

The proposed reliability model for PV farms is presented, in detail, in Section 4. The multi-state reliabil-

$$\lambda = \begin{bmatrix} 0.6991 & 0.2663 & 0.0213 & 0.0053 & 0.0080 & 0 & 0 \\ 0.1755 & 0.5135 & 0.2266 & 0.0706 & 0.0111 & 0.0027 & 0 \\ 0.0254 & 0.2516 & 0.4037 & 0.1903 & 0.1078 & 0.0201 & 0.0011 \\ 0.0099 & 0.1176 & 0.3212 & 0.1440 & 0.1656 & 0.2003 & 0.0414 \\ 0.0116 & 0.0252 & 0.1818 & 0.2805 & 0.0967 & 0.1044 & 0.2998 \\ 0.0024 & 0.0048 & 0.0384 & 0.1799 & 0.2326 & 0.0839 & 0.4580 \\ 0 & 0 & 0 & 0.0083 & 0.0337 & 0.0416 & 0.9164 \end{bmatrix}.$$

Box II

Table 2. COPT of the PV system considering only uncertainty in solar radiation.

State	Cap. (MW)	P_i	λ_+ (occ./hr)	λ_- (occ./hr)	f_i (occ./hr)
1	29.8	0.0688	0	0.3009	0.0207
2	26.4	0.1229	0.1755	0.3110	0.0598
3	22.9	0.1080	0.2770	0.3193	0.0644
4	18	0.0689	0.4487	0.4073	0.0590
5	11.6	0.0590	0.4991	0.4042	0.0533
6	5.9	0.0476	0.4581	0.4580	0.0436
7	0	0.5078	0.0836	0	0.0425

Table 3. PV farm complete reliability model.

State	Cap. (MW)	Prob.	Freq. (occ./hr)
1	29.80	0.0688	0.02070
2	26.40	0.1229	0.05979
3	22.90	0.1080	0.06440
4	19.87	1.2e-10	3.6108e-11
5	18.00	0.0689	0.05898
6	17.60	2.1e-10	1.02165e-10
7	15.27	1.8e-10	1.07334e-10
8	12.00	1.2e-10	1.0272e-10
9	11.60	0.0590	0.058015
10	9.93	6.6e-40	1.98594e-40
11	8.80	1.2e-39	5.838e-40
12	7.73	1.0e-10	9.833e-11
13	7.63	1.0e-39	5.963e-40
14	6.00	6.6e-40	5.6496e-40
15	5.90	0.0476	0.04361
16	3.93	8.1e-11	7.42041e-11
17	3.87	5.7e-40	5.60481e-40
18	1.97	4.6e-40	4.21406e-40
19	0	0.5248	2.21607

ity model and the associated COPT of any PV farms can be obtained using the same procedure presented in Sections 3 and 4. The following steps should be followed precisely to form the reliability model of a PV farm:

Step 1: Form the component reliability model of the PV farm as follows:

- Extract the reliability model of a solar cell based on its failure rate and repair/replacement rate, provided by the manufacturer, or using historical data.
- Form the reliability model of branches in PV panels.
- Form the reliability model of sub-arrays using the number of parallel branches in a panel, the number of series panels in a sub-array, the common-mode failure data of panels, and the reliability data of the DC/DC converter.
- Form the reliability model of PV arrays using the number of parallel sub-arrays in an array. The number of states of the arrays model can be reduced by clustering.
- Form the PV farm component reliability model considering the failure of the DC/AC converter and the number of parallel arrays in a farm. The clustering method can be utilized in this step to reduce the number of states in the PV farm model.

Step 2: Model the uncertainty associated with the solar radiation:

- Determine the output power of the PV farm using the solar radiation data.
- Cluster the output power of the PV farm as segments of the rated power, and calculate the associated state probabilities and transition rates.

Step 3: Form the complete reliability model of the PV farm by combining the component reliability model obtained in Step 1 with the Markov model associated with the uncertainty of solar radiation formed in Step 2.

Using the proposed reliability model, the PV farms can be modeled as a conventional unit with derated power states. Therefore, the analytical generation reliability assessment methods [17] can be utilized for adequacy assessment of the system. In the first stage, the PV farm(s) of the system are modeled and the associated COPT is formed. The obtained COPT is then added to the equivalent COPT of the conventional generating units to form the total generation capacity model of the system. Finally, convolution of the load model with the final COPT provides the risk model of the generation system, and the reliability indices can be calculated.

6. Study results

In this chapter, we present the result of studies performed on two test systems, RBTS [23] and IEEE-RTS [24]. Both systems are modified by adding PV farms, and reliability indices are calculated to investigate the impacts of implementing PV farms. In addition, numerous sensitivity analyses are conducted to investigate the effects of solar radiation average, the penetration level of solar generation and peak load value on the reliability indices.

6.1. Reliability analysis of the RBTS

In this study, the RBTS with 11 generating units is considered [23]. The system load duration curve is

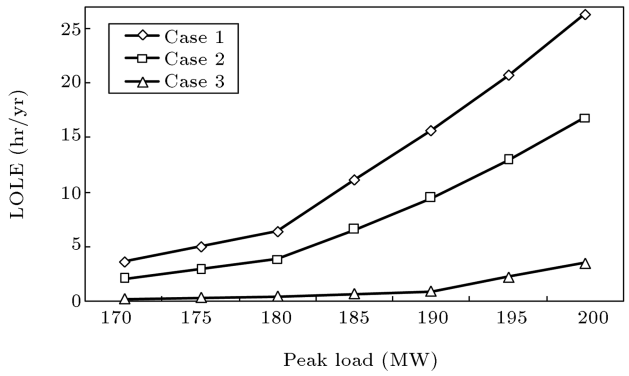

Figure 6. LOLE (hr/yr) versus peak load.

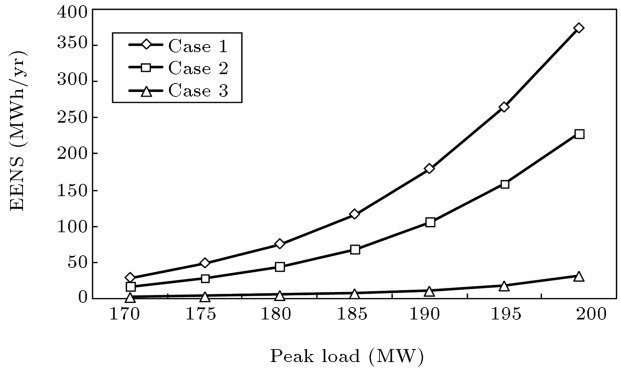

Figure 7. EENS (MWh/yr) versus peak load.

modeled by a straight line from 100% to 60% of the peak load. Three case studies are conducted on the system. In case 1, the basic RBTS is considered. In case 2, a 30 MW PV farm, with the model presented in Section 4, is added to the RBTS. In this case, the 19-state model of Table 3 is simplified to a 7-state model by omitting all states whose probability is less than 10^{-5}. In case 3, a 30 MW conventional generating unit with FOR of 0.02 f/yr is added to the RBTS. The Loss Of Load Expectation (LOLE) and the Expected Energy Not Supplied (EENS) indices for the three cases are presented in Figures 6 and 7, considering different load levels. It can be seen from the results that adding the PV farm in case 2 improves both reliability indices compared to case 1. However, the improvement in reliability indices of case 2 is much lower than the obtained results in case 3, in which a conventional generating unit, with the same size, is added to the system. This is due to the fact that the output of the PV farm is subjected to the solar radiation uncertainty and, therefore, it does not provide all the 30 MW all the time. Besides, it can be seen from the figures that the difference between reliability improvements in cases 2 and 3 increases as the peak load of the system is increased. In order to estimate the capacity value of the 30 MW PV farm in the system, the capacity of the conventional unit that is equivalent to the PV farm and can satisfy the same EENS value is calculated. The

Table 4. Reliability indices versus average solar radiation.

Average solar radiation (w/m^2)	LOLE (hrs/yr)	EENS (MWh/yr)
256	6.93	71.05
276	6.78	69.88
296	6.61	68.92
316	6.54	67.53
336	6.44	67.09
356	6.36	66.41
376	6.31	65.87

Table 5. Impacts of penetration level of PV farms on reliability indices of the IEEE-RTS.

Number of additional 30 MW PV units	LOLE (hrs/yr)	EENS (hrs/yr)
0	112.9	16983.9
1	107.2	16111.0
2	102.6	15342.6
3	98.1	14509.7
4	93.7	13811.4
5	90.0	13465.7

calculations indicate that the equivalent conventional unit capacity of the 30 MW PV farm is 6.17 MW at the peak load of 185 MW. The impacts of average solar radiation on the reliability indices of case 2 are studied in Table 4. The original average solar radiation in the Jask region, which was utilized to construct the reliability model of the 30 MW PV farm, is 316 w/m^2. The reliability model of the PV farm is reconstructed for the six other levels of average solar radiation given in Table 4, and the associated LOLE and EENS indices are calculated and presented in the same table. The peak load of the system is considered to be 185 MW, in this study. It can be seen from Table 4 that both the indices decrease as the average solar radiation increases. This result implies that the construction of PV farms in locations with high solar radiation provides higher reliability benefits.

6.2. Reliability analysis of the IEEE-RTS

The impacts of including large PV farms on the IEEE-RTS test system [24] are studied in this section. The load of this system is modeled by a load duration curve, which is considered to be a straight line from 100% to 60% of the system peak load of 2850 MW. In order to show the impact of the penetration level of the PV farms on the adequacy of the IEEE-RTS, five 30 MW PV farms are continually added to the IEEE-RTS generation system, and the calculated LOLE and EENS indices are presented in Table 5. The PV farms

Table 6. IPLCC of cases 1 and 2 (MW).

Number of added units	1	2	3	4	5
IPLCC(MW) case 1	8.1	16.0	23.8	31.8	39.6
IPLCC(MW) case 2	28.2	56.4	84.6	112.8	140.9

are modeled in the calculations by the same reliability model utilized in the RBTS study. It can be seen from Table 5 that the increase in the penetration level of the PV farms results in additional improvements in the reliability indices.

In order to compare the reliability impact of implementing PV farms with that of adding conventional generating units with the same size, the amount of increment in Peak Load Carrying Capability (IPLCC), due to the addition of the PV farms and conventional units, iscalculated. The IPLCC for cases 1 and 2 are presented in Table 6. It can be seen from the results that addition of the first 30 MW PV farm increases the peak load carrying capability of the system by 8.1 MW, while the addition of the conventional unit with the same size increases PLCC by 28.2 MW. This result shows that the capacity benefit of the PV farm, with the given solar radiation data, is about 29% of a conventional unit with the same size.

7. Conclusion

An analytical method for adequacy assessment of power generation systems, including large PV farms, is proposed in this paper. A reliability model is developed for PV farms, considering both the uncertainties associated with solar radiation and component outages. The proposed reliability model represents a PV farm via a multi-state generating unit, which makes it easy to be utilized in the generation system reliability assessment. The developed model is then utilized to assess the impacts of large PV farm integration on the adequacy of power generation systems. A typical 30 MW PV farm has been considered in the studies, and the proposed model has been utilized to form its reliability model. Real solar radiation data related to the Jask region in the southern part of Iran are utilized in the studies. In the studies performed on the RBTS and the IEEE-RTS, it has been shown that implementing large PV farms improves the adequacy indices of a power generation system. Improvement in the indices significantly increases as the average solar radiation increases. This result highlights the importance of the availability of high solar radiation in the performance and benefits of large PV farms. Finally, it has been shown that the capacity value of the 30 MW PV farm, in the RBTS, with the given data, is about 6 MW, from the view point of power generation adequacy studies. This result indicates that, compared to conventional units of the same size, a less reliable power system is expected when a PV farm is added, if its environmental benefits and low cost operation are not considered. In future work, other economic studies can be done to verify the potential profitability of PV farms, when they are operated combined with other more reliable generation units.

References

1. Wiser, R. and Barbose, G. "Renewables portfolio standards in the United States: A status report with data through 2007", Lawrence Berkeley National Laboratory, Report LBNL 154-E (2008)
2. Regional Greenhouse Gas Initiative (RGGI) "Overview of RGGI CO_2 budget trading program" (Oct. 2007).
3. European Union (EU), *Climate Change: Commission Welcomes Final Adoption of Europe's Climate and Energy Package*, Press Release, EU (Dec. 17, 2008).
4. PV-resources "Large-scale photovoltaic power plants ranking 1-50", http://www.pvresources.com/ PVPowerPlants/Top50.aspx, Accessed 4 April 2013 (2013).
5. Moharil, R.M. and Kulkarni, P.S. "Reliability analysis of solar photovoltaic system using hourly mean solar radiation data", *Solar Energy*, **84**(4), pp. 691-702 (April 2010).
6. Billinton, R. and Bagen, B. "Generating capacity adequacy evaluation of small stand-alone power systems containing solar energy", *Reliability Engineering & System Safety*, **91**(4), pp. 438-443 (April 2006).
7. Billinton, R. and Karki, R. "Capacity expansion of small isolated power systems using PV and wind energy", *IEEE Trans. Power Syst.*, **16**(4), pp. 892-897 (Nov. 2001).
8. Karki, R. and Billinton, R. "Reliability/cost implications of PV and wind energy utilization in small isolated power systems", *IEEE Trans. Energy Conversion*, **16**(4), pp. 368-373 (Dec. 2001).
9. Pradhan, N. and Karki, N.R. "Probabilistic reliability evaluation of off-grid small hybrid solar PV-wind power system for the rural electrification in Nepal", *North American Power Symposium (NAPS)* (2012).
10. Kishore, L.N. and Fernandez, E. "Reliability well-being assessment of PV-wind hybrid system using Monte Carlo simulation", *International Conference on Emerging Trends in Electrical and Computer Technology (ICETECT)* (2011).
11. Burgio, A., Menniti, D., Pinnarelli, A. and Sorrentino, N. "Reliability studies of a PV-WG hybrid system in presence of multi-micro storage systems", *IEEE Conference on Power Technology*, Bucharest (2009).
12. Khaligh, A. and Onar, O.C., *Energy Harvesting, Solar, Wind and Ocean Energy Conversion Systems*, CRC Press (2010).

13. Ramon, S. "A guide to photovoltaic system design and installation", Prepared by California Energy Commission, Energy Technology Development Division, EndeconEngineering, Version 1.0 (June 14, 2001).

14. Wenham, S.R., Green, M.A., Watt, M.E. and Corkish, R., *Applied Photovoltaics*, ARC Centre for Advanced Silicon Photovoltaics and Photonics, UK and USA (2007).

15. Billinton, R. and Allan, R.N., *Reliability Evaluation of Engineering Systems*, 2nd Edition, Plenum Press (1992).

16. *Military Handbook Reliability Prediction of Electronic Equipment*, MIL-HDBK 217F NOTICE 2 (Feb. 1995).

17. Billinton, R. and Allan, R.N., *Reliability Evaluation of Power Systems*, 2nd Edition, Plenum Press, New York and London (1994).

18. Sayas, F.C. and Allan, R.N. "Generation availability assessment of wind farms", *Proc. IEE Gen., Trans., Dist.*, **143**(5), pp. 507-518 (Sep. 1996).

19. Leite, A.P., Borges, C.L.T. and Falcão, D.M. "Probabilistic wind farms generation model for reliability studies applied to Brazilian sites", *IEEE Trans. Power Syst.*, **21**(4), pp. 1493-1501 (Nov. 2006).

20. Suna Sun Data of Jask. http://www.suna.org.ir/fa/ationoffice/windenergyoffi ce/windamar. Accessed 21 June 2012 (2012).

21. Yong Yung, Shuying Huang "Image segmentation by fuzzy c means clustering algorithm with a novel penalty term", *Journal on Computing and Informatics*, **26**(1), pp. 17-31 (2007).

22. Cannon, R.L., Jitendra, V.D. and Bezdek, J.C. "Efficient implementation of the fuzzy c-means clustering algorithms", *IEEE Trans. Pattern Analysis and Machine Intelligence*, PAMI-**8**, no. 2, pp. 248-255 (March 1986).

23. Billinton, R. and Li, W., *Reliability Assessment of Electric Power Systems Using Monte Carlo Methods*, IEEE Press, New York (1991).

24. Grigg, C. "The IEEE reliability test system - 1996", *IEEE Trans. Power Syst.*, **14**(3), pp. 1010-1020 (Aug. 1999).

Biographies

Amir Ghaedi was born in Shiraz, Iran, in 1984. He received his BS degree in Power Engineering from Shiraz University, Iran, in 2007, and MS and PhD degrees in Electrical Engineering from Sharif University of Technology, Tehran, Iran, in 2008, and 2013, respectively. His main research interests are renewable energy, reliability studies and power systems operation.

Ali Abbaspour received BS and MS degrees in Electrical Engineering from Amir Kabir University of Technology, and Tehran University, Iran, respectively, and a PhD degree in Electrical Engineering from Massachusetts Institute of Technology (MIT), USA. Presently, he is Associate Professor in the Department of Electrical Engineering at Sharif University of Technology, Tehran, Iran. Dr. Abbaspour is a member of the Center of Excellence in Power System Control and Management.

Mahmud Fotuhi-Firuzabad received BS and MS degrees in Electrical Engineering from Sharif University of Technology, and Tehran University, Iran, in 1986 and 1989, respectively, and MS and PhD degrees in Electrical Engineering from the University of Saskatchewan, Canada, in 1993 and 1997, respectively. Presently, he is Professor and Head of the Department of Electrical Engineering in Sharif University of Technology, Tehran, Iran. Dr. Fotuhi-Firuzabad is a member of the Center of Excellence in Power System Control and Management, and serves as Editor of the IEEE Transactions on smart grids.

Masood Parvania received a BS degree in Electrical Engineering from Iran University of Science and Technology (IUST), Tehran, Iran, in 2007, and MS and PhD degrees in Electrical Engineering from Sharif University of Technology, Tehran, Iran, in 2009 and 2013, respectively.

Since 2012, he has been Research Associate in the Robert W. Galvin Center for Electricity Innovation at Illinois Institute of Technology, Chicago, IL, USA, and is currently a Postdoctoral Research Fellow in the Electrical Engineering Department at Sharif University of Technology, Tehran, Iran. His research interests include power system reliability and security assessment, as well as operation and optimization of smart electricity grids. He received the Nationwide Distinguished PhD Student Award from the Ministry of Science, Research and Technology of Iran in 2013.